Journal of Applied Polymer Science

Preparation of a Low-Phosphorous Terpolymer as a Scale, Corrosion Inhibitor, and Dispersant for Ferric Oxide

Yiyi Chen,[1] Yuming Zhou,[1] Qingzhao Yao,[1] Yunyun Bu,[1] Huchuan Wang,[1] Wendao Wu,[2] Wei Sun[2]
[1]School of Chemistry and Chemical Engineering, Southeast University, Nanjing 211189, Jiangsu, People's Republic of China
[2]Jianghai Environmental Protection Co., Ltd, Changzhou 213116, Jiangsu, People's Republic of China
Correspondence to: Y. Zhou (E-mail: ymzhou@seu.edu.cn) and Q. Yao (E-mail: 101006377@seu.edu.cn)

ABSTRACT: A novel low-phosphorus terpolymer, used as scale, corrosion inhibitor, and dispersant for iron oxide, was prepared through free-radical polymerization reaction of acrylic acid (AA), oxalic acid-allypolyethoxy carboxylate (APEM), and phosphorous acid (H_3PO_3) in water with redox system of hypophosphorous and ammonium persulfate as initiator. Structure of the synthesized AA-APEM-H_3PO_3 terpolymer was characterized by Fourier transform infrared spectrometer and ^{1}H-NMR. The polymer possesses excellent scale inhibition performance for $CaCO_3$, outstanding ability to disperse ferric oxide, and good corrosion inhibition properties. The study showed that AA-APEM-H_3PO_3 exhibited excellent ability to control calcium carbonate scale, with approximately 90.16% $CaCO_3$ inhibition at a level of 8 mg/L AA-APEM-H_3PO_3. The data of the light transmittance showed that, compared to hydrolyzed polymaleic acid and polyepoxysuccinic acid, AA-APEM-H_3PO_3 had superior ability to control iron ions scaling. The light transmittance of the solution was about 24.1% in the presence of the terpolymer when the dosage was 8 mg/L. Moreover, the corrosion inhibition efficiency could reach up to 79.77% at a dosage of 30 mg/L, with ethylene diamine tetra methylene phosphonic acid just 39.62%. Scanning electronic microscopy, transmission electron microscope, and X-ray powder diffraction analysis were used to investigate the effect of AA-APEM-H_3PO_3 on morphology of calcium carbonate scale. The low-phosphorous terpolymer has also been proven to be effective inhibitor of calcium carbonate even at increasing solution temperature, pH, and Ca^{2+} concentration. The proposed inhibition mechanism suggests the surface complexation and chelation between the functional groups —P(O) $(OH)_2$, —COOH and Ca^{2+}, with polyethylene glycol segments increasing its solubility in water. © 2014 Wiley Periodicals, Inc. J. Appl. Polym. Sci. **2015**, *132*, 41447.

KEYWORDS: copolymers; morphology; properties and characterization; radical polymerization; synthesis and processing

Received 28 May 2014; accepted 25 August 2014
DOI: 10.1002/app.41447

INTRODUCTION

Calcium carbonate is considered most frequent among the commonly occurring scales with the use of water for cooling purposes which has high temperature and elevated concentration. The problem of scaling poses great challenges from both economical and technical sides, decreasing efficiency of cooling water system and increasing frequency of chemical cleaning. To mitigate this problem, chemical additives, that can retard or prevent scale formation, are used even in very small concentrations. Polymers with several functional groups, phosphonate and carboxylate, are effective inhibitors of calcium carbonate growth, such as 1-hydroxy ethylidine-1-diphosphonic acid (HEDP) and hydrolyzed polymaleic anhydride (HPMA).[1–4] However, HEDP contains high phosphorus which can revert to orthophosphates, being potential nutrients for algae. Polycarboxylic acid, HPMA, has low calcium tolerance and can create insolubilization of polymer complexes in the presence of excessive amounts of calcium.[5,6] Therefore, the current trend for inhibitor usage is to develop low-phosphorous and phosphorus-free polymers, with higher calcium tolerance. On the other hand, the optimization of the recycling-water system requires an all-round understanding of the parameters that govern the operations involved.[7] As a result, the inhibitory factors varying with solution temperature, pH, and concentration of Ca^{2+} should be tested.

Iron-based compounds from feed water, such as $FeCl_3$ and $Fe_2(SO_4)_3$, are main sources of iron in cooling water system while the other source includes corrosion products from pipes and the equipment.[8,9] At low pH values from 3 to 4, the ferrous ions have very high solubility in an aqueous medium and pose no challenges for the system. However, when the pH value increases to 5 or above, the ferrous ions, being oxidized to ferric ions by contacting with air, will go through hydrolysis to form iron hydroxide—$Fe(OH)_3$ or iron oxide—Fe_2O_3, which are

insoluble and may deposit on heat-exchanger surfaces and lead to equipment corrosion.[10] As is known, the existence of iron-compounds in the cooling water system can affect the performance of scale inhibitors, such as polymers of acrylic acids.[11] As a result, excellent scale inhibitors should also be effective for dispersing the iron compounds.

Corrosion, within plants and in reservoirs or on heat transfer surfaces, widely occurs in numerous industrial processes when kinds of equipments and facilities are mainly made of carbon steels and stainless steels in cooling water systems.[12,13] Carbon steel, one of the most commonly used metals in daily life, will corrode under many circumstances, especially the process of chemical cleaning with the use of acids.[14] This problem has been solved through the addition of corrosion inhibitors in the systems, such as inorganic and polyphosphate salt corrosion inhibitors.[15,16] However, these inhibitors will pose many other problems, such as secondary pollution and environmental destruction.[17] Therefore, environmental-friendly "green" chemicals should be the current trend for corrosion inhibitors use.

In the present work, a acrylic acid-oxalic acid-allypolyethoxy carboxylate-phosphorous acid (AA-APEM-H_3PO_3) terpolymer containing low-phosphorous was prepared with water as solvent and redox system of hypophosphorous and ammonium persulfate as initiator by the free-radical polymerization. Energy-dispersive X-ray analysis (EDX) and inductively coupled plasma (ICP) were used to measure the concentration of phosphorus in the synthesized terpolymer. The result of EDX showed that phosphorus content was less than 1.5% (mass percentage) and the precise percentage of phosphorus is 1.26% from the analysis of ICP. Therefore, the low-phosphorus terpolymer is a new environmentally safe cooling water treatment agent. The structure of AA-APEM-H_3PO_3 was characterized by Fourier transform infrared (FTIR) and ^{1}H-NMR. The inhibition efficiency of the low-phosphorus terpolymer toward calcium carbonate scale in the artificial cooling water was studied through static scale inhibition tests with different dosages, solution temperature, pH, and concentration of Ca^{2+}. The mechanism was investigated through determining the morphology and crystal structure by scanning electron microcopy (SEM), transmission electron microscope (TEM), and X-ray diffractometer (XRD), respectively. Moreover, the performance of dispersity and corrosion inhibition was determined under different dosages by transmittance observation or dynamic tests.

EXPERIMENTAL

Chemicals and Reagents

Calcium chloride, sodium bicarbonate, magnesium sulfate, sodium chloride, HCl, aminoform, AA, phosphorous acid (H_3PO_3), and ammonium persulfate used were obtained from Zhongdong Chemical Reagent Co., Ltd. (Nanjing, Jiangsu, People's Republic of China). All the above chemicals were in analytically pure grade without further purification, unless otherwise specified. Commercial inhibitors of hydrolyzed polymaleic acid (HPMA, 600 MW), HEDP (206 MW), polyepoxysuccinic acid (PESA, 1500 MW) and 1,2-diaminoethanetetrakismethylene phosphonic acid (EDTMP, 436 MW) were in technical grade and supplied by Jiangsu Jianghai Chemical Co., Ltd. Deionized water (DI water) was used throughout the experiments.

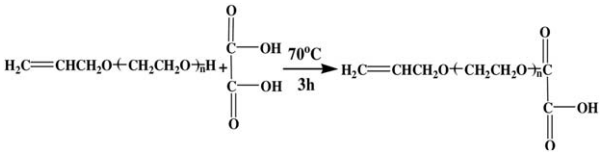

Scheme 1. Synthesis procedure of APEM.

Preparation of AA-APEM-H_3PO_3 Terpolymer

The synthesis procedure of APEM is shown in Scheme 1. APEM was synthesized in our laboratory according to our previous studies.[18] Allyloxy polyethoxy ether (APEG) was carboxylate-terminated using oxalic acid with a molar ratio of 1 : 1. AA was copolymerized with APEM and phosphorous acid (H_3PO_3) in aqueous medium. A 250-mL round-bottom flask equipped with a mechanical stirrer, thermometer, and reflux condenser was charged with 40 mL DI water and a total of 0.5 mol AA and heated to the reaction temperature 80°C over a period of time under nitrogen atmosphere. Then, a definite proportion of APEM and H_3PO_3 were added in 20 mL DI water. In mixed conditions, the initiator ammonium persulfate was dropped at a certain flow rate separately for about 1.5 h. Finally, the low-phosphorus terpolymer AA-APEM-H_3PO_3 was obtained, containing about 23.48% solid. The synthesis procedure of the terpolymer is displayed in Scheme 2.

Characterization of the Synthesized AA-APEM-H_3PO_3

Molecular weight determinations were performed by gel permeation chromatography (GPC, calibrated with PEG standards) with water as the mobile phase at a flow rate of 1.0 mL/min. The structure of AA-APEM-H_3PO_3 terpolymer was analyzed by FTIR spectroscopy (VECTOR-22, Bruker Co., Germany) between 4500 cm^{-1} and 0 cm^{-1}, which was used to confirm the presence of expected functional groups responsible for the scale inhibition property. About 1 mg dried AA-APEM-H_3PO_3 was mixed with 100 mg dried KBr powder and then compressed into a disk for spectrum recording. A Bruker NMR analyzer (AVANCE AV-500, Bruker, Switzerland) was also used to explore the structures of APEG, APEM, and AA-APEM-H_3PO_3, operating at 500 MHz.

Static Scale Inhibition Tests

The inhibition ability of the low-phosphorus AA-APEM-H_3PO_3 terpolymer for calcium carbonate scale was compared with that of the free-inhibitor in flask tests and all inhibitor dosages given below are on a basis of dried conditions.[19] The experiment was

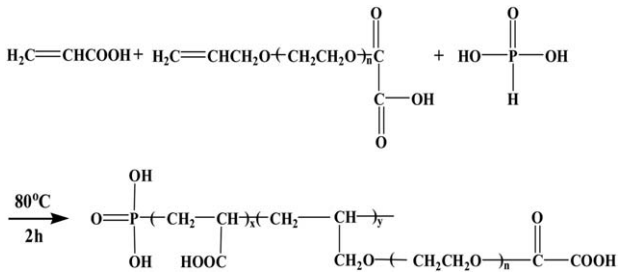

Scheme 2. Synthesis procedure of AA-APEM-H_3PO_3.

carried out in artificial cooling water which was prepared by mixing aqueous solutions of two soluble salts, such as $CaCl_2$ and $NaHCO_3$. Two concentrations of Ca^{2+} and HCO_3^- were 240 mg/L and 732 mg/L, respectively, according to the national standard of People's Republic of China (GB/T 16632-2008). The artificial cooling water containing different quantities of the low-phosphorus terpolymer was heated at 80°C for 10 h in water bath. After that, it was cooled to room temperature. The remaining Ca^{2+} in the supernatant was titrated by EDTA standard solution and compared with blank test. The inhibition efficiency η was defined as:

$$\eta = \frac{\rho 1(Ca^{2+}) - \rho 2(Ca^{2+})}{\rho 0(Ca^{2+}) - \rho 2(Ca^{2+})} \times 100\% \quad (1)$$

where ρ_0 (Ca^{2+}) is the total concentrations of Ca^{2+} (mg/L), ρ_1 (Ca^{2+}) is the concentrations of Ca^{2+} (mg/L) in the presence of the terpolymer inhibitor, ρ_2 (Ca^{2+}) is the concentrations of Ca^{2+} (mg/L) in the absence of the terpolymer inhibitor.

Ability to Disperse Ferric Oxide

The iron dispersing ability of the terpolymer compound was tested through UV–visible studies. Ferrous compounds for the experiment were prepared by adding a known volume of calcium stock solution and iron (II) stock solution to a beaker (1000 mL) with a certain amount of water, at room temperature under continuous stirring, which contained 150 mg/L Ca^{2+} and 10 mg/L Fe^{2+}. The pH value of the solution was adjusted to 9.0 with borax and then the solution was evenly mixed with a known amount of AA-APEM-H_3PO_3 terpolymer. Mixed solution was stirred for 15 min and heated at 50°C for 5 h before being cooled to room temperature. After that, the dispersion performance was evaluated under the wavelength of 420 nm with 722-spectrophotometer by light transmittance.

Corrosion Inhibition Efficiency

The corrosion inhibition efficiency of AA-APEM-H_3PO_3 terpolymer was measured by weight loss of rotating hung steel slices,[20] according to the China National Standard GB/T 18175-2000 for "Performance measurement of corrosion inhibitor in water-treatment with a rotating apparatus." The low carbon steel, used in the experiment, consists of 0.17%–0.23% C, 0.17%–0.37% Si, 0.35%–0.65% Mn, ≤0.25% Cr, ≤0.3% Ni, ≤0.25% Cu, and balance Fe and its surface area is 28.00 cm^2. The 2 L solution, containing 1.11 g of $CaCl_2{\cdot}2H_2O$, 0.896 g of $MgSO_4{\cdot}7H_2O$, 0.336 g of NaCl, and 0.336 g of $NaHCO_3$, was mixed with a known amount of AA-APEM-H_3PO_3 terpolymer. Then the experiments were done under the conditions that the temperature is at 45°C, the rotating speed is 75 RPM, and the testing time is 72 h. The corrosion efficiency was calculated as formulas (2) and (3):

$$X = \frac{87,600 \times [(m_0 - m_1) - \Delta m]}{s \times \rho \times t} \quad (2)$$

$$\eta = \frac{X_0 - X_1}{X_0} \times 100\% \quad (3)$$

where m_0 is the mass of carbon steel hung slices before test; m_1 is the mass of carbon steel hung slices after test; Δm is the mass loss of carbon steel hung slices caused by washing in acid (20% HCl and 8 g/L of aminoform). s is the surface area of carbon steel hung slice (28 cm^2). t is the testing time (72 h). ρ is the density of carbon steel hung slices. X_0 is the annual corrosion rate in the absence of scale inhibitor (mm/y). X_1 is the annual corrosion efficiency in the presence of scale inhibitor (mm/y). η is the corrosion inhibition efficiency (%).

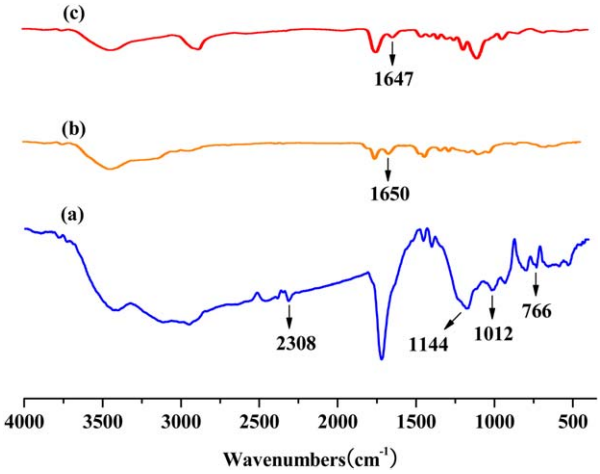

Figure 1. The FTIR spectrum of (a) AA-APEM-H_3PO_3, (b) AA, (c) APEM. [Color figure can be viewed in the online issue, which is available at wileyonlinelibrary.com.]

Morphology Characterization

The morphological change of the $CaCO_3$ crystals on glass plates was examined through SEM, TEM, and XRD, with the addition of the terpolymer. The samples were coated with a layer of gold and observed in a SEM (S-3400N, HITECH). A TEM (JEM-2100SX, Japan) was also used to observe the shape of calcium carbonate crystal. Precipitated phases were identified by XRD on a Rigaku D/max 2400 X-ray powder diffractometer with Cu Kα ($\lambda = 1.5406$) radiation (40 kV, 120 mA).

RESULTS AND DISCUSSIONS

Molecular Weight Determination

The molecular weight is an important parameter in the process of scale inhibition. The weight distribution of the polymer was investigated with gel permeation chromatography (GPC, calibrated with PEG standards) with the 1.0 mL/min run flow rate. The weight-average molecular weight (M_w) of the terpolymer (AA/APEM (2 : 1)) was found to be 17.5k, whereas its number-average molecular weight (M_n) was 16.4k.

Structure Analysis of AA-APEM-H_3PO_3

The FTIR spectra were taken for the synthesized terpolymer (a), raw materials AA (b), and APEM (c), as shown in Figure 1. It is found that there are characteristic absorption peaks of 2308 cm^{-1}, 1144 cm^{-1}, 1012 cm^{-1}, and 766 cm^{-1}, among which the vibration at 2308 cm^{-1} is attributed to P—O_{str}, 1144 cm^{-1} and 1012 cm^{-1} is attributed to P═O_{str}, and most importantly, 766 cm^{-1} is attributed to P—C_{def}.[3] The peaks that appear at 1650 cm^{-1} and 1647 cm^{-1} in curves (b) and (c) are for the C═O stretching vibration, while there are no peaks between 1620 cm^{-1} and 1680 cm^{-1} in curve (a), clearly revealing that free radical polymerization among AA, APEM, and H_3PO_3 has occurred successfully. Meanwhile, EDX was used to get information about the elemental composition of the

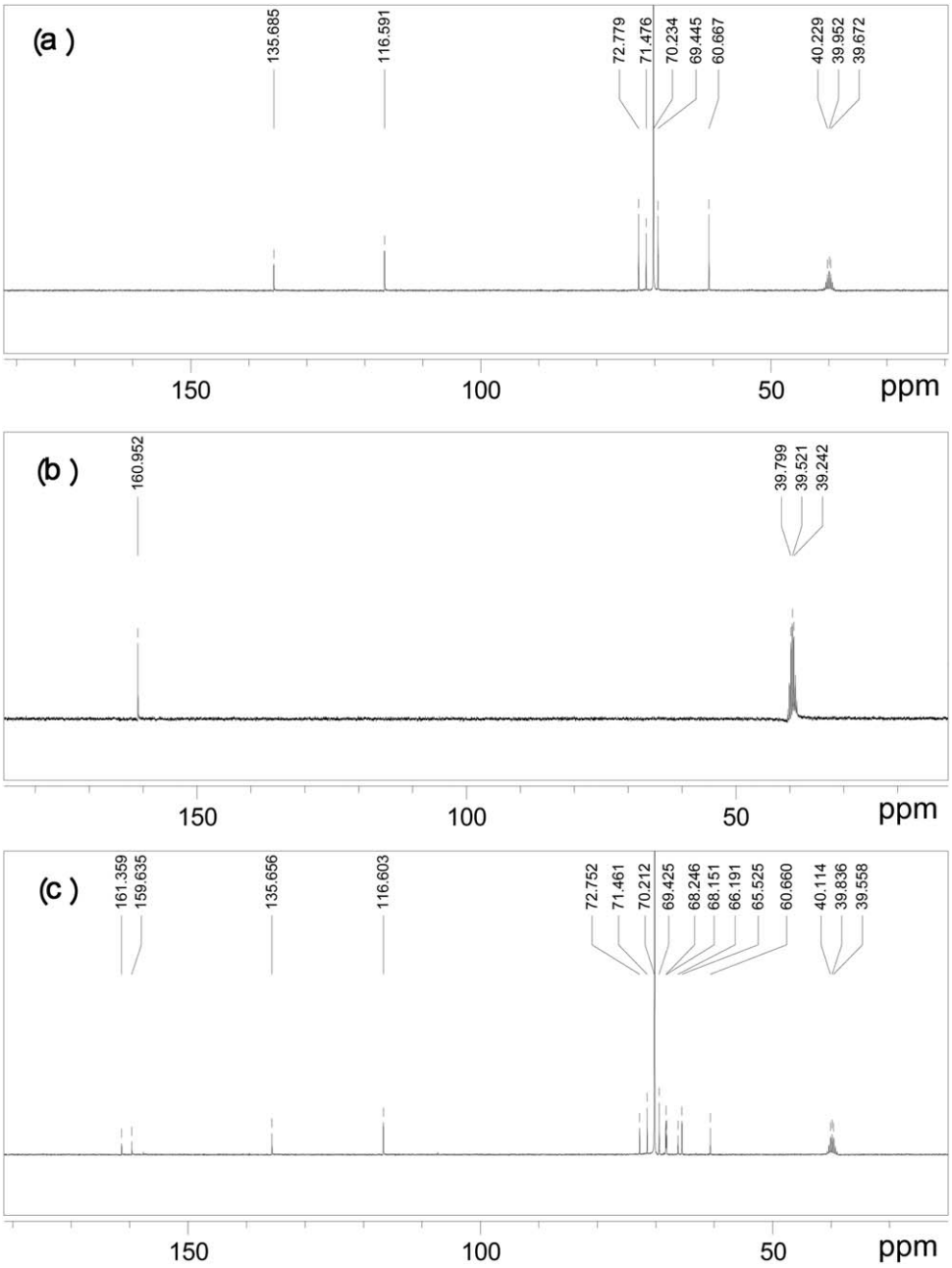

Figure 2. The ^{13}C-NMR spectrum of (a) APEG, (b) oxalic acid, and (c) APEM.

low-phosphorus AA-APEM-H_3PO_3 terpolymer, including C, O, and P. The results show that the phosphorus content is less than 1.5% in weight, which carries the points of low-phosphorus content and environment friendly.

The structure of raw materials and the synthesized terpolymer was characterized by ^{13}C NMR and ^{1}H-NMR with deuterated dimethyl sulfoxide as the solvent and the corresponding spectra are exhibited in Figures 2 and 3, respectively. From Figure 2, there are peaks at 39.6 ppm in those three curves, which are attributed to the solvent residual peak of $(CD_3)_2SO$. The chemical shifts in the region from 60 to 75 ppm are assigned to the ether groups (—CH_2CH_2O—) in Figure 2(a,c). The unique peak at 160.9 ppm in curve (b) is assigned to the carbonyl carbons in oxalic acid molecule. However, in curve (c) the chemical shift has changed to two peaks, 159.6 ppm and 161.4 ppm, between which the former is attributed to the ester group adjacent ethyl group and the latter is assigned to the terminal carboxyl group in APEM. The oxyethyl groups are electron donating groups, which will decrease the chemical shift value of the carbonyl carbons, while the increased chemical shift of the terminal carboxyl group is attributed to the left electron withdrawing group-the ester group. This fact reveals that the active hydroxyl group of APEG has reacted with oxalic acid.

According to the data in Figure 3, the peak at 2.50 is also assigned to the solvent residual peak of $(CD_3)_2SO$. The chemical

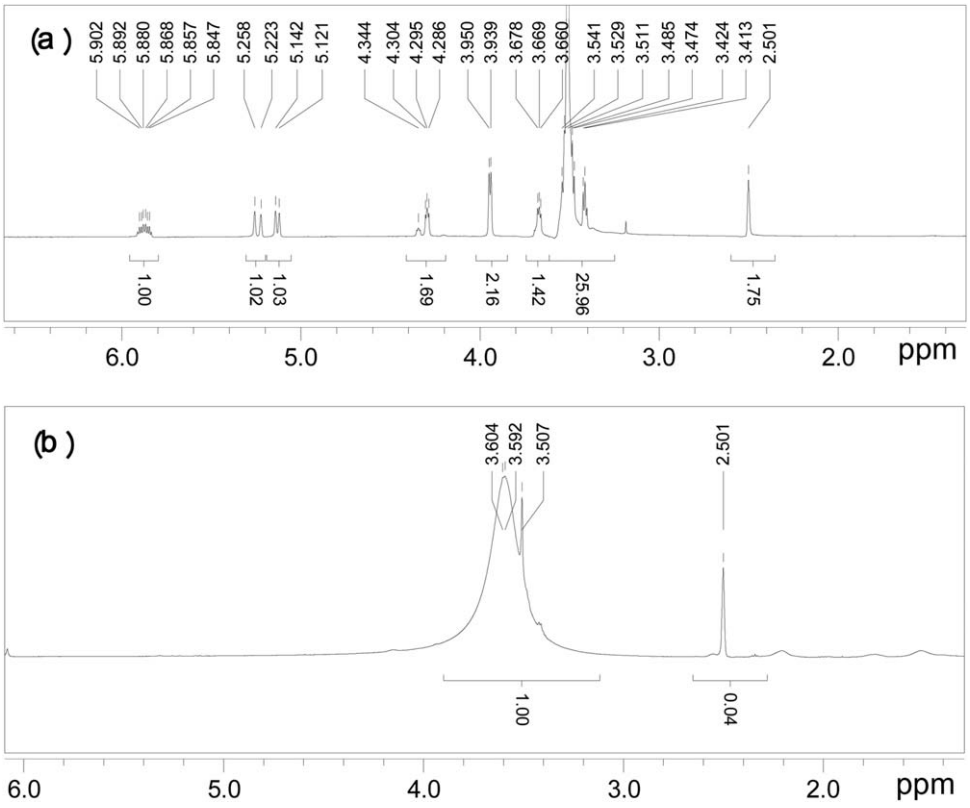

Figure 3. The ^{1}H-NMR spectrum of (a) APEM and (b) AA-APEM-H_3PO_3.

shift in the region from 4 ppm to 6 ppm are assigned to propenyl protons (CH_2═CH─CH_2─) in curve (a), while there are no peaks in this range in curve (b). In this case, the double bond absorption peaks completely disappear, revealing that the free radical polymerization among AA and APEM has occurred,[18] which is corresponding to the result of FTIR analysis.

After the analysis from FTIR and NMR above, the low-phosphorus terpolymer AA-APEM-H_3PO_3 has been synthesized as expected.

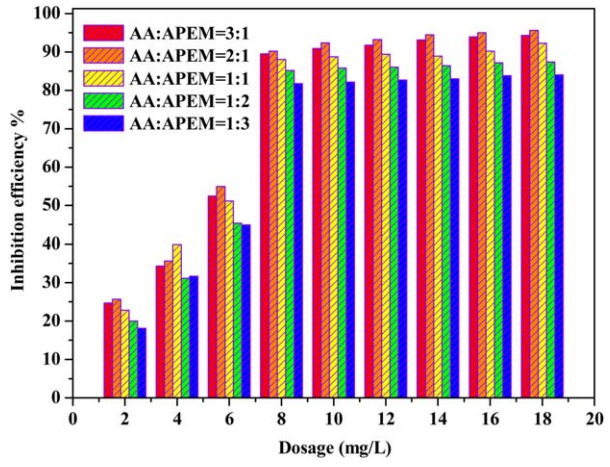

Figure 4. The influence of AA/APEM mole ratio on calcium carbonate scale inhibition. [Color figure can be viewed in the online issue, which is available at wileyonlinelibrary.com.]

The Relationship Between AA/APEM Mole Ratio and the Calcium Carbonate Scale Inhibition Efficiency

The ability of AA-APEM-H_3PO_3 to control $CaCO_3$ deposits was prepared at different AA/APEM mole ratio with fixed amount of phosphorous acid, as shown in Figure 4. According to the data, the terpolymers show pool anti-scaling performance at 2 mg/L dosage and there are sudden increases as the concentrations increase from 2 mg/L to 8 mg/L. In particular, under the same experimental conditions, the inhibition efficiency obtained for AA/APEM (2 : 1) is about 90.16% at a level of 8 mg/L polymer and they are about 89.46%, 88.03%, 85.14%, and 81.77% for AA/APEM (3 : 1), AA/APEM (1 : 1), AA/APEM (1 : 2), and AA/APEM (1 : 3), respectively. It is obvious that when the mole ratio of AA and APEM is 2 : 1, the terpolymer shows the best anti-scaling performance.

The Relationship Between AA-APEM-H_3PO_3 Concentration and the Calcium Carbonate Scale Inhibition Efficiency

The effect of the terpolymer (AA/APEM (2 : 1)) as an inhibitor for calcium carbonate was compared with that of other scale inhibitors, HPMA, HEDP, and AA-APEM (2 : 1), as shown in Figure 5. All the data in Figure 5 show that the ability to control calcium carbonate precipitation followed the order AA-APEM-H_3PO_3 > AA-APEM > HEDP > HPMA. As is apparent from Figure 5, the concentration of AA-APEM-H_3PO_3 strongly affects its performance on calcium carbonate inhibition and the terpolymer exhibits an obvious threshold effect. Scale inhibition effect increases with the increasing concentration of the terpolymer when the terpolymer concentration is below

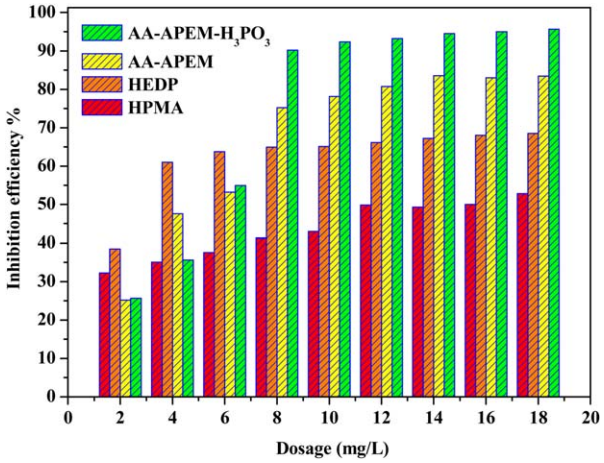

Figure 5. Inhibition on calcium carbonate as a function of inhibitor dosage. [Color figure can be viewed in the online issue, which is available at wileyonlinelibrary.com.]

8 mg/L. Namely after the concentration exceeds about 8 mg/L, the inhibition efficiency does not obviously increase with the increasing concentrations.[18,21] Compared to AA-APEM, a copolymer without phosphorous acid end group, AA-APEM-H_3PO_3 still has superior ability on the inhibition of calcium carbonate deposits, with 90.16% inhibition at a level of 8 mg/L, whereas it is 76.20% for AA-APEM at the same dosage. This fact indicates that the phosphorous acid groups have some effect on the anti-scaling performance. It is also worth mentioning that phosphonates, such as HEDP, an effective inhibitor on calcium carbonate deposits, displays significant ability to control calcium carbonate scales and its inhibition is superior to that of the other investigated nonphosphorus inhibitor, HPMA, which only contains carboxyl groups and can hardly control calcium carbonate scales even at a high dosage, as is apparent from Figure 5. Therefore, it can be seen from Figure 5 that the inhibitor AA-APEM-H_3PO_3 (AA/APEM (2 : 1)) displays the best ability to control calcium carbonate scales among those inhibitors investigated, namely, HPMA, HEDP, and AA-APEM (2 : 1).

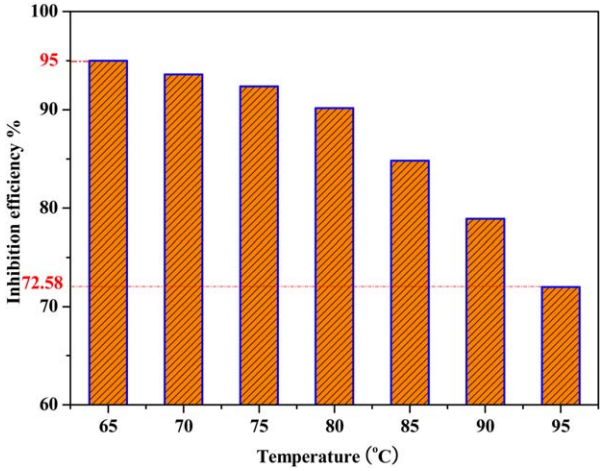

Figure 6. The influence of temperature on calcium carbonate scale inhibition at a level of 8 mg/L AA-APEM-H_3PO_3. [Color figure can be viewed in the online issue, which is available at wileyonlinelibrary.com.]

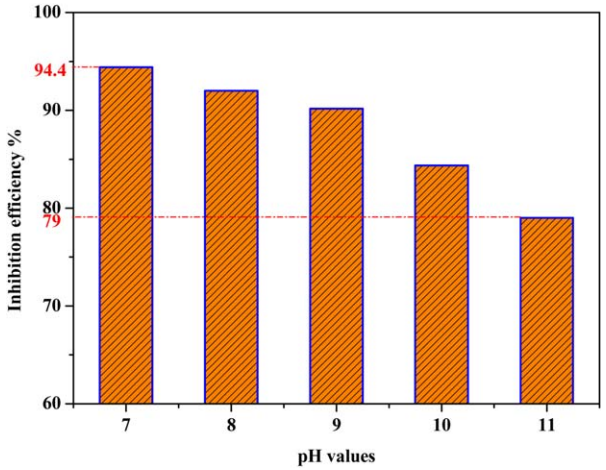

Figure 7. The influence of pH on calcium carbonate scale inhibition at a level of 8 mg/L AA-APEM-H_3PO_3. [Color figure can be viewed in the online issue, which is available at wileyonlinelibrary.com.]

This conclusion suggests that the phosphonate groups of phosphorous acid, the side-chain polyethylene glycol (PEG) segments of APEM and carboxyl groups of AA might play an important role during the control of calcium carbonate deposits.

The Relationship Between Test Temperature and the Calcium Carbonate Scale Inhibition Efficiency

The experiments were to study the patterns of how test temperature affected the scale inhibition performance when taking AA-APEM-H_3PO_3 (AA/APEM (2 : 1)) as scale inhibitor, and setting the pH of the water sample to 9.0 and the concentration of Ca^{2+} to 240 mg/L (counted by $CaCO_3$). Results are shown in Figure 6.

It can be found that temperature has a big effect on calcium carbonate scale inhibition and they are in a linear decreasing trend with the raise of temperature from Figure 6. When the temperature raises from 65°C to 95°C, the corresponding efficiency decreases from 95% to 72.58%, about 20% loss in calcium carbonate inhibition. However, the inhibition efficiency is still above 70%, which indicates the superior thermal stability of the terpolymer and that it can still work at a high temperature. This can be ascribed that the solubility of calcium carbonate decreases when increasing the temperature.

The Relationship Between pH and the Calcium Carbonate Scale Inhibition Efficiency

The experiments studied the influencing rules of pH value on the calcium carbonate scale inhibition by AA-APEM-H_3PO_3 (AA/APEM (2 : 1)) when the solution temperature was 80°C and the concentration of Ca^{2+} was 240 mg/L. The results are shown in Figure 7 as follows.

As illustrated in Figure 7, calcium carbonate inhibitory power drops from 94.4% to 79% with the increase of pH value of the solution from 7.0 to 11.0, which indicates that the scale inhibition efficiency to $CaCO_3$ is influenced greatly by the system acidity. As is known that with the increase of pH, the concentration of OH^- increases and the equilibrium between OH^- and H^+ breaks up, leading to the decrease of H^+,[22] the direct

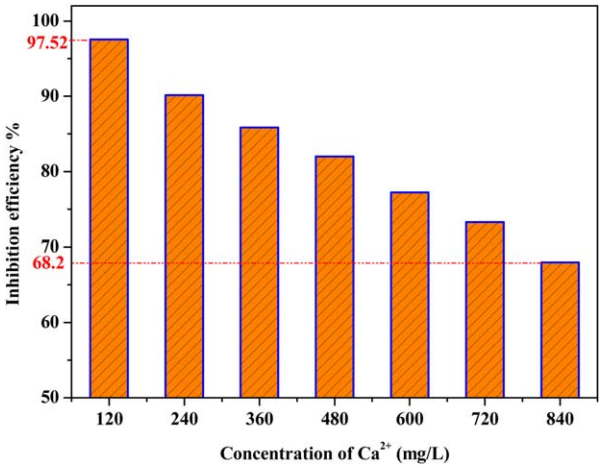

Figure 8. The influence of concentration of Ca^{2+} on calcium carbonate scale inhibition at a level of 8 mg/L AA-APEM-H_3PO_3. [Color figure can be viewed in the online issue, which is available at wileyonlinelibrary.com.]

result is that calcium carbonate precipitation forms easily and the scale inhibition declines.[13] At a pH of 8.8–9.2, the usual pH values of the industry recycling water, the terpolymer still shows superior calcium carbonate inhibition.

The Relationship Between Concentrations of Ca^{2+} and the Calcium Carbonate Scale Inhibition Efficiency

The temperature and pH value of the scale inhibition system was 80°C and 9.0, respectively. The influencing rules of the concentration of Ca^{2+} (hardness of the water) on the scale inhibition were conducted in this experiment and the results are shown in Figure 8.

The data in Figure 8 show that the scale inhibition efficiency of the terpolymer (AA/APEM (2 : 1)) gradually decreases with the increase in the concentration of Ca^{2+}. When increasing the concentration of Ca^{2+} from 120 mg/L to 840 mg/L, the inhibitory power decreases from 97.52% to 68.2%. This trend of scale inhibition is easy to understand that the hardness of the water is an essential factor on scale inhibition test. What should be emphasized is that the calcium carbonate scale inhibition is still higher than 60% even when the hardness value is 840 mg/L.

Table I. Ferric Oxide Dispersion of AA-APEM-H_3PO_3, HPMA, and PESA

Dosage (mg/L)	Light Transmittance (%) with		
	AA-APEM-H_3PO_3	HPMA	PESA
0	100	100	100
2	92.4	94.2	96.7
4	65.7	88.4	88.9
6	36.4	82.6	91.3
8	24.1	81.3	87.2
10	28.8	85.8	85.6
12	24.7	82.1	83.6
14	21.2	84.0	82.1
16	20.3	86.6	87.4

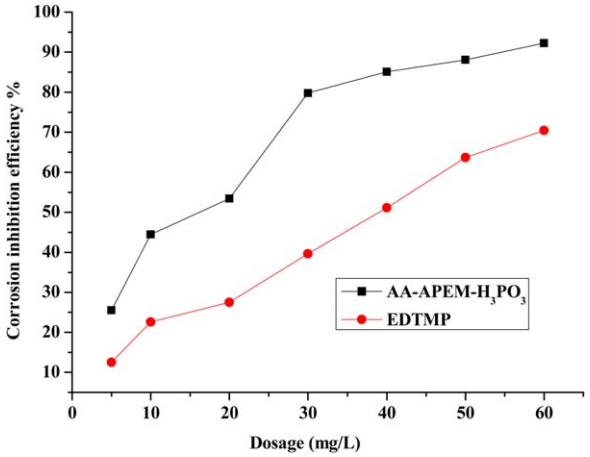

Figure 9. Corrosion inhibition efficiency of AA-APEM-H_3PO_3 as a function of inhibitor dosage. [Color figure can be viewed in the online issue, which is available at wileyonlinelibrary.com.]

Ability of AA-APEM-H_3PO_3 to Disperse Ferric Oxide

The effect of the terpolymer (AA/APEM (2 : 1)) on dispersion to ferric oxide is presented in Table I, compared with commercial polymers, HPMA and PESA. As shown in Table I, the iron dispersancy of the terpolymer is much better than that of HPMA and PESA. It is disclosed that the transmittance ratio to disperse ferric oxide reduces along with the increase of AA-APEM-H_3PO_3 dosage from 0 to 16 mg/L and the best transmittance ratio is 20.3%, while HPMA and PESA display hardly any dispersancy. This fact demonstrates that the PEG groups on AA-APEM-H_3PO_3 matrix play an important role on dispersion to ferric oxide.

Corrosion Inhibition Efficiency of AA-APEM-H_3PO_3 Terpolymer

The effect of the concentration of the terpolymer (AA/APEM (2 : 1)) on corrosion inhibition performance was compared with a commercial corrosion inhibitor, EDTMP, as shown in Figure 9. The photographs, showing the changes of carbon steels with addition of AA-APEM-H_3PO_3, are also depicted in Figure 10. Figure 9 illustrates that AA-APEM-H_3PO_3 has a good effect on the corrosion inhibition, because the efficiency increases to 79.77% when the concentration is just 30 mg/L while the efficiency of EDTMP is only 39.62% at the same concentration. As is also apparent from Figure 10, in the absence of inhibitor, the steel sample seems very rough on the surface while the rough surface is disappeared with the addition of inhibitor. These phenomena may attribute to the functional groups, —$P(O)(OH)_2$, which can form an unsaturated heterocyclic structure with π-bonds and lone electron pairs. Then the charge will urge the inhibitor to adsorb on the carbon steel surface and protect the carbon steels.[23,24]

SEM Analysis of $CaCO_3$ Crystal

SEM is one of the widely used nondestructive surface examination techniques. The change of crystal size and modifications, brought about by the low-phosphorus terpolymer AA-APEM-H_3PO_3 addition, was examined through SEM.

The morphology of collected $CaCO_3$ crystal obtained in the absence and presence of 2, 6, 8 mg/L terpolymer are shown in

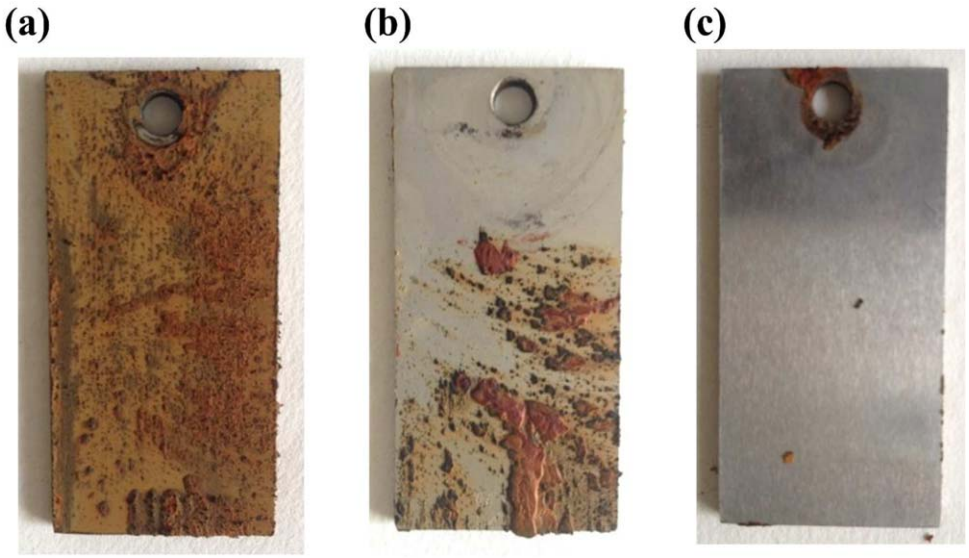

Figure 10. Photographs of the changes of carbon steels in the presence of AA-APEM-H_3PO_3 at levels of (a) 0 mg/L, (b) 20 mg/L and (c) 50 mg/L. [Color figure can be viewed in the online issue, which is available at wileyonlinelibrary.com.]

Figure 11. Three occurring mineral phases, calcite, aragonite, and vaterite, could be clearly distinguished by their characteristic morphologies.[25] Figure 11(a) reveals that calcium carbonate scales are mainly calcite scales, which are symmetry and block-like particles of cubic shape or rhombohedra. Variations in the calcite crystal morphology and the crystal sizes are observed in the presence of the low-phosphorus terpolymer AA-APEM-H_3PO_3. Figure 11(b) illustrates that the regular shaped structure is damaged and it seems that the crystal is split into a great many needles, which is the primary shape feature of aragonite. When the concentration is 6 mg/L, oblate spherical shape particles are visible in the SEM image [Figure 11(c)]. There are lots of vaterite phases being more dispersive, which are broken into pieces and set into the bunch crystal with higher concentration. In this case, the deposition will be easily removed with enough shear force from flowing water.[26] The low-phosphorus

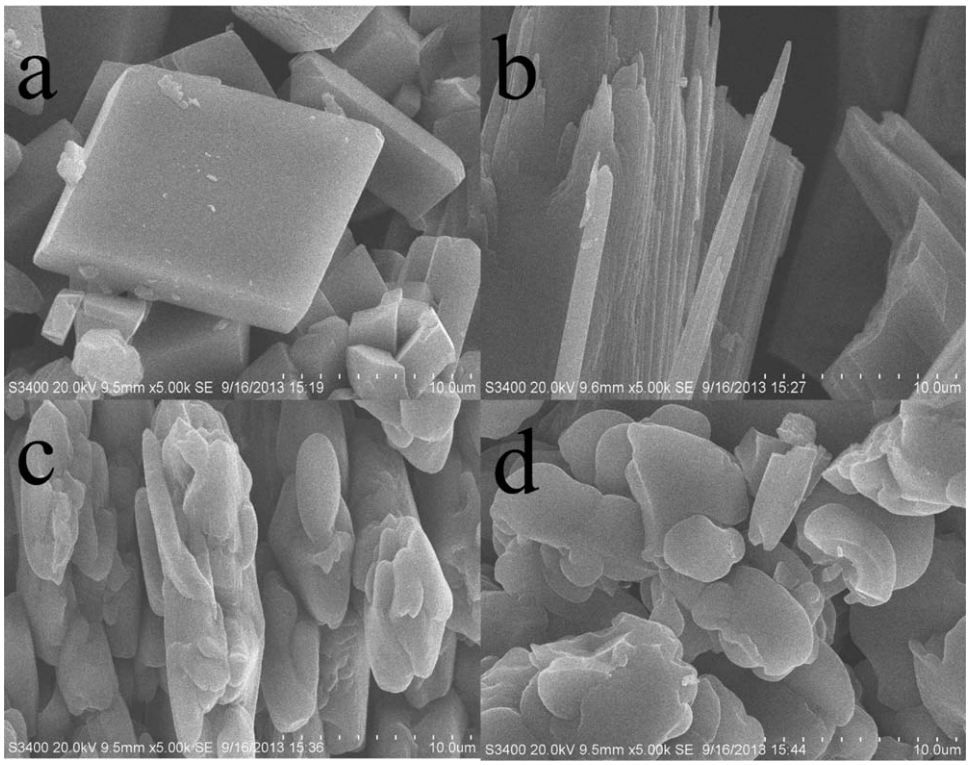

Figure 11. SEM images for the calcium carbonate (a), with the presence of 2 mg/L (b), 6 mg/L (c), and 8 mg/L (d) AA-APEM-H_3PO_3.

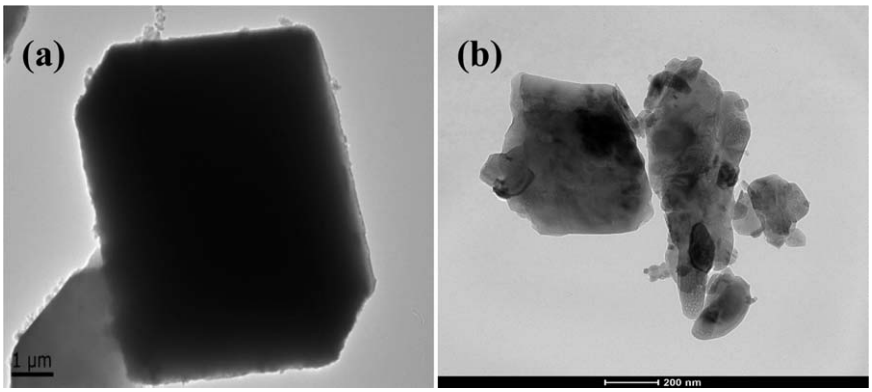

Figure 12. TEM images for the calcium carbonate (a), with the presence of 6 mg/L (b) AA-APEM-H_3PO_3.

terpolymer AA-APEM-H_3PO_3 dramatically changed the morphology of the calcite crystals, probably due to the strong specific interaction between crystals and functional groups, which are —P(O)$(OH)_2$, —COOH, and PEG groups. The initial step is surface complexation of the negatively charged polydentate ligand through its carboxylate or phosphonate moieties onto the positively charged Ca^{2+} lattice ions. In fact, the phosphonate group is doubly deprotonated so that the —P(O)$(OH)_2$ moiety bridges two Ca^{2+} centers. A part of the phosphonate group and the neighboring carboxylate group oxygen atoms at the PAA segments form a seven-membered chelate with the Ca^{2+} center, while the other part chelates Ca^{2+} with several carbonyl moieties in other molecule chains.[27] As a consequence, the structure of crystals can be significantly distorted and weakened, as shown in Figure 11.

TEM Analysis of $CaCO_3$ Crystal

Figure 12 shows the TEM micrographs of calcium carbonate in the absence [Figure 12(a)] and in the presence [Figure 12(b)] of AA-APEM-H_3PO_3. As shown in Figure 12(a), regular shaped rhombohedral crystal, characteristic of calcite, was obtained without addition of the terpolymer. However, with the addition of 6 mg/L AA-APEM-H_3PO_3, calcium carbonate scales become much looser and softer and the decrescent particles are distributed randomly, as shown in Figure 12(b). This illustrates that the low-phosphorous terpolymer can prevent the precipitation of calcium carbonate effectively.

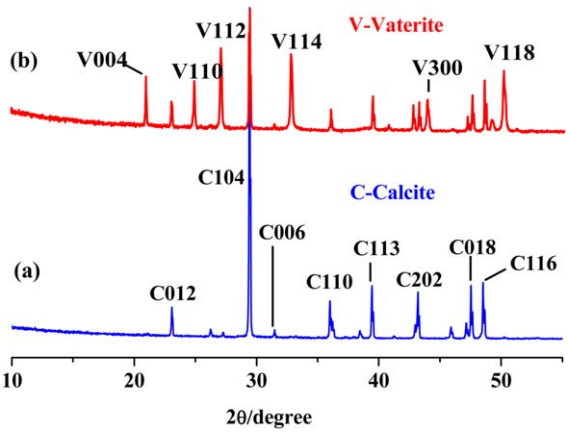

Figure 13. The XRD pattern of the calcium carbonate crystals. (a)Without the low-phosphorus terpolymer and (b) with the low-phosphorus terpolymer. [Color figure can be viewed in the online issue, which is available at wileyonlinelibrary.com.]

XRD Analysis of $CaCO_3$ Crystal

To examine the scale structural changes in calcium carbonate in the presence and absence of the low-phosphorus terpolymer, the means of XRD was also used and the result is shown in Figure 13. In the absence of the low-phosphorous terpolymer, it can be inferred that the structure is calcite, which is the main crystal form of calcium carbonate, according to the 2θ values. Figure 13(b) shows that with the addition of terpolymer, there are (004), (110), (112), (114), (300), and (118) strong peaks corresponding to vaterite, which is another form of calcium carbonate and the least stable.[18] These results indicate that the synthesized AA-APEM-H_3PO_3 could inhibit or disturb the calcite growth and induce vaterite growth, which is harder to adhere to metal surface and easy to disperse in water solution.[28]

CONCLUSIONS

A low-phosphorus terpolymer AA-APEM-H_3PO_3 has been synthesized, characterized, and evaluated successfully. FTIR and ^{1}H-NMR identify that AA-APEM-H_3PO_3 had the expected structure and the phosphorus content was less than 1.5% in weight with the use of EDX. AA-APEM-H_3PO_3 was employed as an excellent scale and corrosion inhibitor and a dispersant. The results of static scale inhibition tests showed that the terpolymer was effective in the calcium carbonate scale inhibition and exhibited nearly 90.16% of $CaCO_3$ at a threshold dosage of 8 mg/L. SEM, TEM, and XRD analysis of calcium carbonate scale suggest the changes in the crystal size and morphology. Moreover, the sharp falling in light transmittance from 92.4% to 24.1% was recorded when the threshold dosage of 8 mg/L was applied and this revealed that AA-APEM-H_3PO_3 was an effective dispersant. Besides, the method of rotating hung steel slices was used and it has been found that the low-phosphorous terpolymer had good corrosion inhibition ability. These are all because it simultaneously possesses phosphonate and carboxylate groups.

No reference to the low-phosphorus terpolymer AA-APEM-H_3PO_3 used as calcium carbonate scale inhibitor, dispersant for ferric oxide, and corrosion inhibitor in cooling water systems

has been found in the literature, it is believed to represent a potentially new environmental water treatment agent.

ACKNOWLEDGMENTS

This work was supported by the Prospective Joint Research Project of Jiangsu Province (BY2012196); the National Natural Science Foundation of China (51077013); special funds for Jiangsu Province Scientific and Technological Achievements Projects of China (BA2011086); the Fundamental Research Funds for the Central Universities; Scientific Innovation Research Foundation of College Graduate in Jiangsu Province (CXLX13-107); program for Training of 333 High-Level Talent, Jiangsu Province of China (BRA2010033).

REFERENCES

1. Kavitha, A. L.; Vasudevan, T.; Prabu, H. G. *Desalination* **2011**, *268*, 38.
2. Shen, Z. H.; Li, J. S.; Xu, K.; Ding, L. L.; Ren, H. Q. *Desalination* **2012**, *284*, 238.
3. Wang, C.; Li, S. P.; Li, T. D. *Desalination* **2009**, *249*, 1.
4. Wang, H. C.; Zhou, Y. M.; Yao, Q. Z.; Ma, S. S.; Wu, W. D.; Sun, W. *Desalination* **2014**, *340*, 1.
5. Tsortos, A.; Nancollas, G. H. *J. Colloid Interface Sci.* **2002**, *250*, 159.
6. Amjad, Z. *Colloid Surf.* **1990**, *48*, 95.
7. Fu, C. E.; Zhou, Y. M.; Xie, H. T. *Ind. Eng. Chem. Res.* **2010**, *49*, 8920.
8. Liang, Z.; Wang, Y. X.; Zhou, Y.; Liu, H.; Wu, Z. B. *Water Environ. Res.* **2009**, *81*, 2293.
9. Matilainen, A.; Lindqvist, N.; Tuhkanen, T. *Environ. Technol.* **2005**, *26*, 867.
10. Lakshmanan, D.; Clifford, D. A.; Samanta, G. *Environ. Sci. Technol.* **2009**, *43*, 3853.
11. Fu, C. E.; Zhou, Y. M.; Xie, H. T.; Sun, W.; Wu, W. D. *Ind. Eng. Chem. Res.* **2010**, *49*, 8920.
12. Touira, R.; Dkhirechea, N.; Ebn Touhami, M.; Sfaira, M.; Senhaji, O.; Robin, J. J.; Boutevin, B.; Cherkaoui, M. *Mater. Chem. Phys.* **2010**, *122*, 1.
13. Zhang, H. X.; Wang, F.; Jin, X. H.; Zhu, Y. C. *Desalination* **2013**, *236*, 55.
14. Mayakrishnan, G.; Nagamani, S.; Devarayan, K.; Ick, S. K.; Ramasamy, K. *Ind. Eng. Chem. Res.* **2012**, *51*, 7910.
15. Dyer, S. J.; Anderson, C. E.; Graham, G. M. *J. Pet. Sci. Eng.* **2004**, *43*, 259.
16. Bougeard, C. M. M.; Goslan, E. H.; Jefferson, B.; Parsons, S. A. *Water Res.* **2010**, *44*, 729.
17. Touir, R.; Dkhireche, N.; Ebn Touhami, M.; Lakhrissi, M.; Lakhrissi, B.; Sfaira, M. *Desalination* **2009**, *249*, 922.
18. Chen, Y. Y.; Zhou, Y. M.; Yao, Q. Z.; Bu, Y. Y.; Wang, H. C.; Wu, W. D.; Sun, W. *Desal. Wat. Treat.* DOI: 10.1080/19443994.2014.922500.
19. Liu, G. Q.; Huang, J. Y.; Zhou, Y. M.; Yao, Q. Z.; Ling, L.; Zhang, P. X.; Wang, H. C.; Cao, K.; Liu, Y. H.; Wu, W. D.; Sun, W.; Hu, H. J. *Tenside Surfactants Deterg.* **2012**, *5*, 404.
20. Xu, Y.; Zhang, B.; Zhao, L. L.; Cui, Y. C. *Desalination* **2013**, *311*, 156.
21. Shakkthivel, P.; Vasudevan, T. *Desalination* **2006**, *197*, 179.
22. Qiang, X.; Sheng, Z.; Zhang, H. *Desalination* **2013**, *309*, 237.
23. Wang, H. C.; Zhou, Y. M.; Liu, G. Q.; Huang, J. Y.; Yao, Q. Z.; Ma, S. S.; Cao, K.; Liu, Y. H.; Tian, Y. J.; Wu, W. D.; Sun, W.; Hu, Z. J. *Tenside Surfactants Deterg.* **2014**, *51*, 248.
24. Zhang, B.; Zhou, D. P.; Lv, X. G.; Xu, Y.; Cui, Y. C. *Desalination* **2013**, *327*, 32.
25. Nehrke, G.; Van Cappellen, P. *J. Cryst. Growth* **2006**, *287*, 528.
26. Jing, G. L.; Li, X. X. *Appl. Sci. Eng. Technol.* **2013**, *6*, 3372.
27. Demadis, K. D.; Lykoudis, P.; Raptis, R. G.; Mezei, G. *Cryst. Growth Des.* **2006**, *6*, 1064.
28. Chen, T.; Neville, A.; Sorbie, K.; Zhong, Z. *Chem. Eng. Sci.* **2009**, *64*, 912.